Cell

Structural Evolution of Glycan Recognition by a Family of Potent HIV Antibodies

Fernando Garces,[1,2,3,10] Devin Sok,[2,3,4,9,10] Leopold Kong,[1,2,3] Ryan McBride,[5] Helen J. Kim,[1] Karen F. Saye-Francisco,[2,3,4] Jean-Philippe Julien,[1,2,3] Yuanzi Hua,[1] Albert Cupo,[7] John P. Moore,[7] James C. Paulson,[5] Andrew B. Ward,[1,2,3] Dennis R. Burton,[2,3,4,8,*] and Ian A. Wilson[1,2,3,6,*]

[1]Department of Integrative Structural and Computational Biology
[2]International AIDS Vaccine Initiative Neutralizing Antibody Center
[3]Scripps Center for HIV/AIDS Vaccine Immunology & Immunogen Discovery
[4]Department of Immunology and Microbial Science
[5]Department of Cell and Molecular Biology
[6]Skaggs Institute for Chemical Biology
The Scripps Research Institute, La Jolla, CA 92037, USA
[7]Department of Microbiology and Immunology, Weill Medical College of Cornell University, New York, NY 10021, USA
[8]Ragon Institute of MGH, MIT, and Harvard, Cambridge, MA 02139, USA
[9]International AIDS Vaccine Initiative, New York, NY 10038, USA
[10]Co-first author
*Correspondence: burton@scripps.edu (D.R.B.), wilson@scripps.edu (I.A.W.)
http://dx.doi.org/10.1016/j.cell.2014.09.009

SUMMARY

The HIV envelope glycoprotein (Env) is densely covered with self-glycans that should help shield it from recognition by the human immune system. Here, we examine how a particularly potent family of broadly neutralizing antibodies (Abs) has evolved common and distinct structural features to counter the glycan shield and interact with both glycan and protein components of HIV Env. The inferred germline antibody already harbors potential binding pockets for a glycan and a short protein segment. Affinity maturation then leads to divergent evolutionary branches that either focus on a single glycan and protein segment (e.g., Ab PGT124) or engage multiple glycans (e.g., Abs PGT121–123). Furthermore, other surrounding glycans are avoided by selecting an appropriate initial antibody shape that prevents steric hindrance. Such molecular recognition lessons are important for engineering proteins that can recognize or accommodate glycans.

INTRODUCTION

The HIV-1 envelope glycoprotein (Env) trimer is the sole target of the neutralizing antibody response and the primary platform for vaccine design. However, variable loops on gp120 mediate antibody escape, and extensive N-linked glycosylation shields much of the Env protein surface from immune recognition. Additionally, many antibodies against monomeric gp120 bind without measurable glycan involvement or show enhanced binding following deglycosylation (Binley et al., 1998; Koch et al., 2003; Ma et al., 2011). Notwithstanding, a number of potent broadly neutralizing antibodies (bnAbs) have recently been discovered that bind to a heavily glycosylated region around the base of the V3 loop that we have termed a supersite of vulnerability (Kong et al., 2013). These bnAbs include antibody families from different germline lineages such as PGT121–123/PGT133–134/10-1074, PGT125–128/PGT130–131, and PGT135–137 (Julien et al., 2013c; Kong et al., 2013; Mouquet et al., 2012; Pejchal et al., 2011; Walker et al., 2011). Crystal structures of PGT128 and PGT135 in complex with gp120 outer domain and with gp120 core, respectively, and PGT122 in complex with the soluble cleaved BG505 SOSIP.664 gp140 trimer (SOSIP.664) (Julien et al., 2013a, 2013b; Kong et al., 2013; Pejchal et al., 2011) have enabled molecular characterization of their glycan-dependent bnAb epitopes. Although these bnAbs are derived from different germline lineages, they all interact with the Asn332 (N332) glycan that is highly conserved across the majority of HIV-1 isolates. In addition, PGT128 binds the glycan at Asn301 (N301) and the base of the gp120 V3 loop, PGT135 interacts with glycans at Asn386 (N386) and Asn392 (N392) and an extensive β sheet motif on the gp120 outer domain, and PGT122 contacts glycans at N301, Asn137 (N137), and Asn156 (N156), as well as protein components of the V1 and V3 loops. A family of trimer-preferring antibodies, PG9/PG16, also recognizes N156 in V1 but interacts with a glycan in V2, Asn160 (N160) at the trimer apex (Julien et al., 2013a; McLellan et al., 2011). A common feature of these antibodies is interaction with multiple glycans and protein components to achieve high affinity. Indeed, these same bnAbs generally have low or undetectable affinity to single glycans (McLellan et al., 2011; Mouquet et al., 2012). For carbohydrate-binding lectins, high affinities that are relevant in vivo are achieved through interaction with multiple glycans (Dam et al., 2000). Only

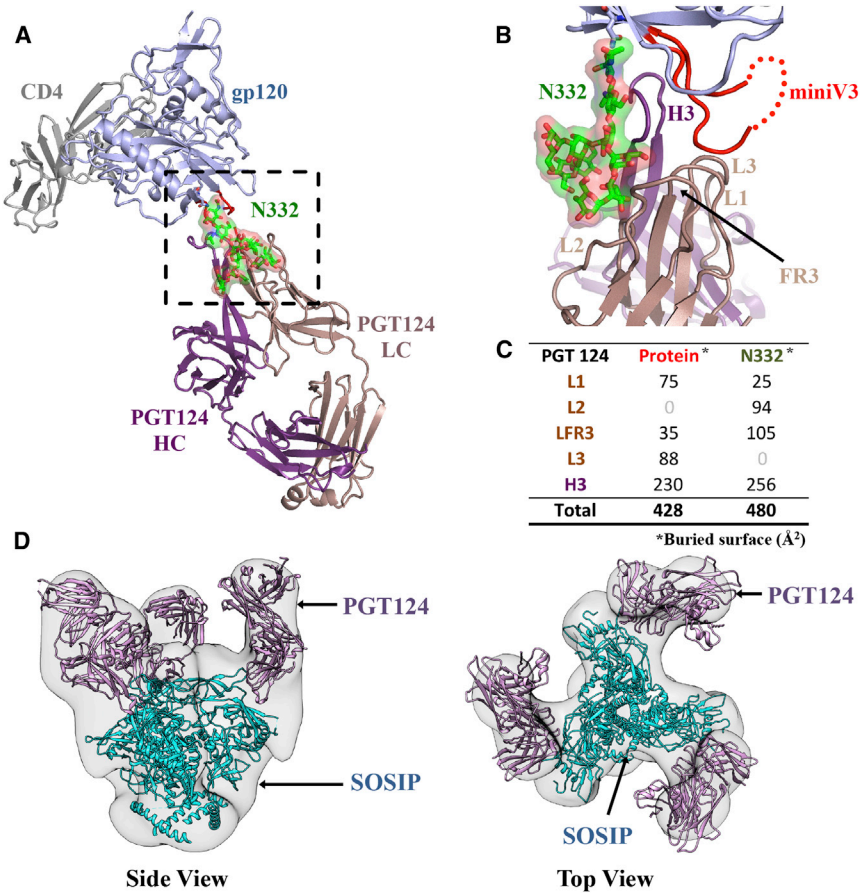

Figure 1. Crystal Structure of PGT124 in Complex with HIV-1 gp120 and CD4

(A) The ternary complex of PGT124 (purple and brown for heavy and light chains, respectively) and two-domain CD4 (gray) bound to gp120 (light blue) are shown as a ribbon representation. PGT124 contacts the N332 glycan and the base of V3. The glycan is represented in ball and stick with green carbons, red oxygens, and blue nitrogens and covered with its molecular surface.

(B) CDR H3, L1, L2, and L3 loops and the light-chain FR3 make extensive contacts with both the Man_8 N332 glycan and V3 (in red) of gp120.

(C) The surface areas (Å^2) buried on the gp120 protein and N332 glycan by individual CDR loops and framework regions on PGT124 are presented on the lower right.

(D) Fitting of the PGT122-BG505 SOSIP.664 gp140 crystal structure into the PGT124:BG505 SOSIP EM reconstruction at 17.8 Å resolution. The PGT122 fitting is excellent with a correlation of 0.9, indicating that PGT122 and PGT124 share a similar angle of approach for interaction with Env (see also Figures S1 and S2 and Tables S1 and S6).

one HIV-1 antibody, 2G12, has been able to attain high affinity for glycans alone by using multivalency through domain swapping of the variable heavy chain (V_H) domains, whereby two tightly linked Fabs then bind multiple glycans in the N332 high mannose patch (Calarese et al., 2003). To achieve high-affinity binding without multivalency, a combination of glycan and protein interactions would appear to be a more general solution.

PGT122 is a member of the PGT121 family of bnAbs, which are among the most potent antibodies identified to date. Passively administered PGT121 protects against mucosal SHIV (chimeric simian HIV) challenge in macaques at serum concentrations achievable by vaccination and causes a dramatic and sustained lowering of viral load in established SHIV infection (Moldt et al., 2012; Barouch et al., 2013). The crystal structure of BG505 SOSIP.664 with PGT122 revealed how an affinity-matured antibody from the PGT121 family recognizes gp120 in the context of the Env trimer (Julien et al., 2013a). PGT124 is a newly discovered bnAb from the same germline lineage as PGT121 but represents an alternative branch in the antibody maturation process and is 89% identical in V_H amino acid sequence to 10-1074 (Figure S1C available online) (Mouquet et al., 2012; Sok et al., 2013, 2014).

Structural comparison of representatives from these two different evolutionary branches therefore provides an opportunity to investigate the evolution of high-affinity recognition of an epitope involving glycans and protein surfaces. Molecular details of the PGT124-gp120 interaction were determined by X-ray crystallography and EM, with additional functional and biochemical insights from isothermal titration calorimetry (ITC), next-generation sequencing, virus neutralization, and glycan arrays. Surprisingly, PGT124 engages in a distinct mode of interaction with the N332 supersite of vulnerability that involves a single glycan, whereas PGT122 contacts multiple glycans.

RESULTS

Structural Characterization of PGT124 in Complex with gp120 and CD4

To identify the PGT124 epitope, we cocrystallized PGT124 Fab in complex with a gp120 core containing a mini-V3 loop (mV3) (Pejchal et al., 2011). The JRCSF gp120 mV3 core was produced in a *GnTI*$^{-/-}$ mutant cell line that yields $Man_{5\text{-}9}GlcNAc_2$ oligomannose glycans (Chang et al., 2007; Reeves et al., 2002). The complex was deglycosylated by Endoglycosidase H (EndoH) to remove glycans not protected by PGT124 binding, and two-domain soluble CD4 was added to facilitate crystallization. The crystal structure was determined at 3.3 Å with four ternary complexes in the asymmetric unit (Tables S1 and S6).

The most prominent interaction of PGT124 with gp120 is with a single $Man_8GlcNAc_2$ glycan (Man_8) linked to N332 and a small protein segment at the V3 loop base (Figures 1A and 1B). Structurally, both protein and glycan components make comparable contributions to the PGT124 epitope, as the bnAb buries 428 Å^2 of gp120 polypeptide and 480 Å^2 of N332 Man_8 glycan (Figure 1C). Whereas the N332 glycan was protected from EndoH deglycosylation by the antibody prior to crystallization,

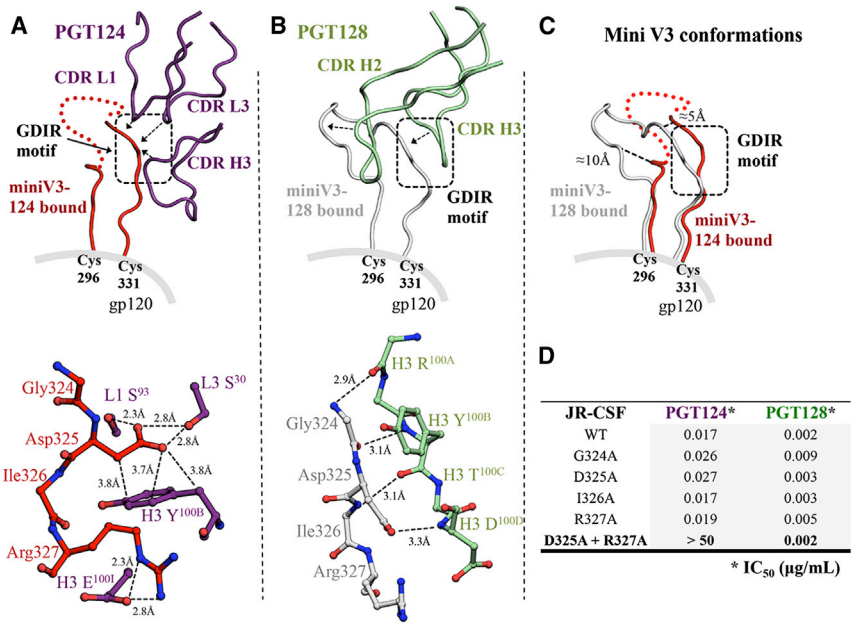

D

JR-CSF	PGT124*	PGT128*
WT	0.017	0.002
G324A	0.026	0.009
D325A	0.027	0.003
I326A	0.017	0.003
R327A	0.019	0.005
D325A + R327A	**> 50**	**0.002**

* IC_{50} (μg/mL)

Figure 2. Interaction between PGT124 and the Base of the V3 Loop

(A) The interaction between PGT124 CDR loops (purple ribbons) and the base of the V3 loop (red ribbon). Red dots represent residues at the tip of the mini-V3 loop that are not visible in the electron density. The interaction with contacting residues is displayed in ball-and-stick representation below. Contacts between side chains of the ^{324}GDIR^{327} motif on the V3 loop and the CDR loops of PGT124 are indicated with solid lines for van der Waals' interactions and dotted lines for hydrogen bonds.

(B) For comparison, the interaction between PGT128 CDR loops (pale green) and the base of the V3 (gray) (PDB 3TYG) for comparison with (A). The PGT128 antibody-antigen interactions with the V3 base are all H bonds of the Fab main chain with V3 main chain.

(C) The V3 loop structures bound to PGT124 or PGT128 are superimposed for comparison.

(D) The effect on the neutralization activity of PGT124 and PGT128 by single and double mutations of the V3 loop GDIR motif. Values are shown as IC_{50} in μg/ml (see also Figures S3, S4, and S5).

most other glycans appear to be cleaved, as indicated by electron density for only single *N*-acetylglucosamine (GlcNAc) moieties at N262, N276, N295, N301, N339, N355, N386, N392, N411, and N448. Thus, it is unlikely that the N301 glycan near the base of V3 makes productive contacts with PGT124. However, additional electron density at N295 and N339 could be assigned to two core GlcNAcs (data not shown) in one of the four copies in the asymmetric unit, suggesting partial protection from cleavage by EndoH. Electron density for gp120 was mostly unambiguous except for the mV3 tip, which is disordered. However, the V3 base is highly ordered as PGT124 makes its only contacts with the gp120 polypeptide in this region (Figure 2A). Superposition of the unliganded PGT124 structure at 2.5 Å (Table S1) with its bound form gave an all-atom root mean square deviation (rmsd) of 0.6 Å, indicating no major changes in the antibody on gp120 binding (Figure S1A).

To characterize the PGT124 interaction in the context of the SOSIP.664 Env trimer (Depetris et al., 2012; Sanders et al., 2002), we derived negative-stain electron microscopy (EM) images at 17.8 Å resolution. Three Fabs are bound per trimer with each oriented diagonally relative to the trimer axis (Figure S2A). The PGT122:SOSIP.664 crystal structure (PDB ID:4NCO) fits extremely well into the PGT124:SOSIP.664 EM reconstruction, indicating that both bnAbs approach Env at a similar angle (Figure 1D).

Molecular Basis of PGT124 Recognition of gp120 Polypeptide

PGT124 recognizes the ^{324}GDIR^{327} region at the V3 loop base. As other N332-dependent antibodies, including PGT128, bind this same sequence, this motif may be a common anchor point. For PGT124, Ser^{30} and Ser^{93} in CDR L1 and L3, respectively, interact with the gp120 Asp325 carboxylate (Figure 2A), which is also involved in stacking interactions with CDR H3 Tyr^{100B}. Remarkably, PGT124 utilizes three different CDR loops to target Asp325. Furthermore, a salt bridge is formed between CDR H3 Glu^{100I} and gp120 Arg327. However, these side-chain-mediated PGT124 interactions contrast with the backbone-mediated recognition of the same ^{324}GDIR^{327} region by PGT128, thus highlighting substantial differences in how antibodies from different lineages recognize the same region in an epitope (Figure 2B). Furthermore, Asp325 can be substituted by Asn without affecting PGT124 interaction as HIV-1 isolates such as CNE20 and CAAN5342.A2 with ^{324}GNIR^{327} can be neutralized. This ^{325}D/NxR^{327} motif is 94.1% conserved across HIV-1 strains, as calculated using 3,045 aligned gp120 sequences (Los Alamos HIV Database). As expected, mutation of GDIR to GAIA completely abrogated PGT124 binding to gp120 in an ITC assay (Figures S3A and S3B). A JRCSF pseudovirus variant containing GAIA was poorly neutralized by PGT124 compared to wild-type, whereas the same mutations had no effect on neutralization by PGT128 (Figure 2D). Thus, PGT124 interacts with the highly conserved V3 base in a distinct manner from PGT128. Accordingly, successful elicitation of these two types of bnAbs may require differently designed immunogens.

Further comparison between the PGT124:gp120 core-mV3 and PGT128:ODmV3 (PDBID:3TYG) structures confirmed that the GDIR motif is structurally similar (1.0 Å Cα RMSD), although significant flexibility is observed in the overall V3 loop conformation (2.4 Å Cα RMSD), where the observed ends of the V3 loop shift by 10 Å and 5 Å (Figure 2C). The PGT128 V3 conformation is likely affected by antibody binding, as extensive interactions are also made with the N301 glycan within the mV3.

The PGT124:core-mV3 crystal structure was also compared with the PGT122:SOSIP.664 trimer structure (PDB ID 4NCO), where superposition indicates that the V3 base—and the GDIR motif in particular—adopts similar, but not identical, conformations (Figure S4), suggesting that binding does not substantially perturb the gp120 conformation in monomer or trimer context.

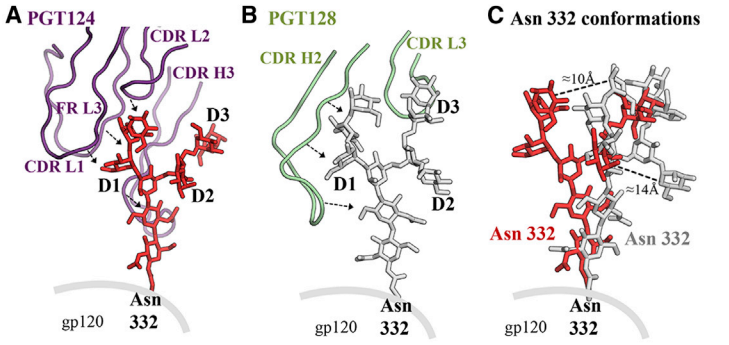

E

	94UG103	92RW020	92BR020	JR-CSF	92TH021	IAVI C22
WT (293T)	0.162	0.001	0.003	0.042	> 50	0.001
GnTI$^{-/-}$ (293S)	0.174	0.006	0.021	0.047	> 50	0.006
+ Kifunensine (293T)	0.276	0.006	0.019	0.034	> 50	0.008
+ Swainsonine (293T)	0.123	0.004	0.009	0.023	> 50	0.004
+ NB-DNJ (293T)	ND	ND	0.011	ND	ND	ND
N332A	**>50**	**>50**	**>50**	**>50**	**>50**	**>50**

IC_{50} (μg/mL)
50
10
1
0.1
0.01
0.001

Figure 3. Interaction between PGT124 and the N332 Glycan

(A) Interaction of the CDR loops of PGT124 in purple with the oligomannose glycan at the N332 position in red ball-and-stick representation with the D1, D2, and D3 arms labeled.

(B) For comparison, the interaction of the PGT128 CDR loops (light green) is shown with the N332 glycan (gray ball-and-stick representation).

(C) The N332 glycan structures bound to PGT128 or PGT124 are shown after superposition of the gp120 protein components. Conformational differences are highlighted by comparative distances between equivalent mannose moieties.

(D) Schematic diagram of the $Man_8GlcNAc_2$ glycan with the glycan moiety nomenclature.

(E) The effect on PGT124 neutralization activity of differences in gp120 glycosylation arising from different cell expression systems and removal of the N332 glycan. Values are shown as IC_{50} in μg/ml (see also Figures S3, S5, and S6 and Tables S2 and S3).

$Man_{8/9}$ Linked to Asn332 Is the Primary PGT124 Glycan Contact in the N332 Supersite of Vulnerability

The PGT124 structure reveals the molecular basis for the highly focused N332 glycan interaction. The antibody engages carbohydrate primarily at the junction of the light (LC) and heavy (HC) chains (Figure 3A) and makes multiple interactions to gp120 via CDR L2, light-chain framework 3 (FR L3), and the 24-residue CDR H3 that forms an extended β hairpin (Figure 3A). The long H3 loop penetrates the glycan shield to reach the gp120 protein surface, and its extended backbone packs along the entire length of the N332 glycan. Additional glycan interactions are made with a pocket formed by CDR L2, FR L3, and CDR H3, where the C-mannose moiety forms hydrogen bonds and van der Waals interactions (Figure 3D). Site-directed alanine mutagenesis confirms that Asn^{L51} and Arg^{H100}, which directly contact the glycan, moderately affect PGT124 neutralization, whereas Ile^{L66b} has a weaker effect (Figure S5). Together, these extensive glycan contacts, in combination with interactions with the GDIR motif, appear to be sufficient to attain high-affinity binding, without engaging other glycans, as with PGT128 and PGT135. Nevertheless, although PGT124 contacts the three mannose moieties on the D1 arm, only two seem to impact neutralization (Figure S5). Moreover, PGT124 can neutralize viruses grown in different cell lines or in the presence of glycosidase inhibitors (Figure 3E), presumably because the N332 glycan composition is not significantly impacted as it is protected from modifying enzymes by the dense oligomannose patch on the gp120 outer domain (Bonomelli et al., 2011).

Cocrystal structures of gp120 with a variety of N332-dependent bnAbs (PGT128 [PDB ID 3TYG], PGT135 [PDB ID 4JM2], and PGT124) allow assessment of the structure and conformational flexibility of the N332 glycan. First, superimposition of their gp120 protein components shows that the D1, D2, and D3 arms of the N332 glycan generally project in the same direction. However, while the PGT135- and PG128-bound N332 glycans vary by only 8° in an arc from each other, the PGT124-bound N332 deviates by 20–25° from its corresponding orientations in the PGT128 and PGT135 complexes, bending closer toward the V3 loop (Figures 3A–3C, S6A, and S6B). Otherwise, the N332 glycan seems to have a rather rigid architecture. Superimposition only on the N332 glycan reveals remarkably good correspondence of the glycan conformation with only slight deviations (Figure S6C) as reflected in all-atom rmsds of 2.5 Å and 2.9 Å for N332-PGT124 versus N332-PGT135 and N332-PGT124 versus N332-PGT128 structures, respectively. Thus, the N332 glycan has a consistent similar general orientation, but antibodies can fix some of the apparently limited conformational heterogeneity. Finally, PGT124 binds a different face of the glycan than PGT135, which interacts with the N332 D2 and D3 arms rather than D1. In contrast, PGT124 contacts the same glycan face as PGT128, which binds the D1 and D3 arms. Consequently, this variation in N332 glycan recognition and binding modes creates specific footprints for each antibody.

Although derived from the same putative germline precursor, PGT124 and PGT122 make different sets of glycan contacts. PGT124 contacts only N332 on the JRCSF gp120 core, whereas PGT122 contacts four different glycans on the BG505 SOSIP.664 trimer (Julien et al., 2013a). Indeed, in the absence of the N332 glycan, PGT122 requires N137 and N301 to neutralize the BG505 virus (Julien et al., 2013a). To determine whether PGT124 also depends on these glycans, we eliminated single glycan sites in the V1/V2 loops and in the high-mannose patch of Env; these changes had little to no effect on PGT124 neutralization (Table S2). Consistent with the structural data, only N332 glycan removal abrogated PGT124 neutralization across a number of isolates (Sok et al., 2014). In contrast, PGT121 exhibits isolate-specific effects in the presence or absence of N332 (Table S2) (Sok et al., 2013), likely reflecting its ability to utilize alternative glycans at either N137 or N301 (Sok et al., 2014). Removal of these glycan sites individually did not affect or even enhance PGT121 activity, implying that each glycan interaction is relatively weak. Thus, it appears that the glycans are recognized in combination with the protein component via a cooperative interaction to achieve a high-affinity interaction. Although PGT124

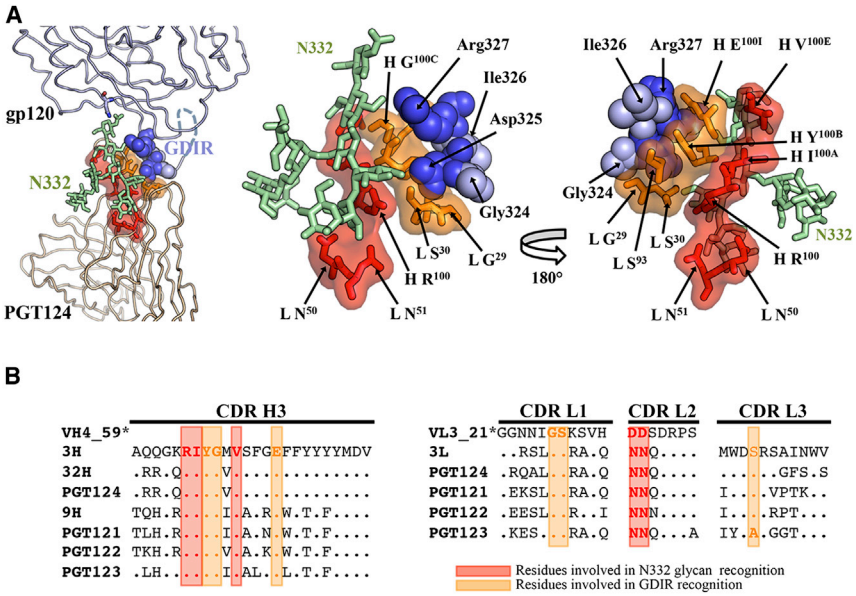

Figure 4. Epitope Core of the PGT121 Germline Lineage

(A) Cartoon representation of the interaction between mV3-gp120 core and the PGT124 variable region (left) and close-up views of the PGT124 epitope core with the ^{324}GDIR^{327} motif at the V3 base in blue spheres and the N332 glycan as pale green ball and stick (middle and right). The PGT124 residues that contact the N332 glycan and the V3 protein motif are represented in red and orange as a ball and stick, respectively, and covered with its molecular surface.

(B) Sequence alignment of heavy and light chains of PGT121–124 Abs and germline precursors (asterisk indicates that the germline CDR L3 and CDR H3 sequences are not used for alignment because of ambiguity associated with D gene assignment). Red and orange boxes indicate that residues that contact the N332 glycan and the GDIR motif, respectively, on the epitope core of PGT124 are also largely conserved in PGT121–123 and, importantly, in the germline sequence (see also Figure S1).

and PGT121/PGT122 derive from the same germline genes and have high structural homology, they have diverged significantly in how they interact with their epitopes centered on the N332 glycan. Nevertheless, the entire constellation of glycans likely dictates the approach angle of these antibodies to the Env trimer where either several (PGT122) glycans or one (PGT124) glycan are contacted and others are avoided.

We previously reported that removal of the N332 glycan abrogates PGT124 neutralization for the overwhelming majority of isolates (Sok et al., 2014). To determine how PGT124 neutralizes HIV in the absence of N332, we investigated a small set of representative isolates (Table S3). Neighboring glycan sites were removed in combination with N332 by alanine mutagenesis, and the double mutants were tested to see whether PGT124 was dependent on them for neutralization. Loss of neutralization was found for removal of N295, N301, N339, and N392 glycan sites in combination with N332 removal, but little to no effect was seen with single mutations (Table S3). Accordingly, for a small subset of viruses, PGT124 is capable of utilizing nearby glycans when N332 is not present (Table S3).

PGT124 Binding Does Not Appear to Be Dependent on Other Surrounding Glycans on the HIV-1 Trimer

PGT124 primarily contacts N332, whereas PGT122 also contacts N137, N156, and N301 (Figure 1) (Julien et al., 2013a). Therefore, we analyzed sequences in this family in the context of known structures to assess the evolution of their binding sites during antibody maturation. Residues in common in PGT122 and PGT124 CDRs mediate contacts to N332 and GDIR (Figure 4). Indeed, almost all of these contact residues are also present in the germline (GL) and are retained in various intermediates (3H, 32H, and 9H for the heavy chain and 3L for the light chain), as well as in the affinity-matured antibodies from different branches of the phylogenetic tree (PGT121–124). Thus, N332 glycan and GDIR recognition appears to be the key event in initiating the antibody response.

Comparison of HIV neutralization by inferred intermediates and affinity-matured antibodies against various glycan mutants reveals considerable complexity in glycan epitope recognition. We therefore focused on the four glycan sites (N137, N156, N301, and N332) that mediate binding of PGT122 to the BG505 isolate. We tested neutralization of antibody 3H+3L, the least-mutated inferred intermediate for this lineage, as well as 32H+3L that is an inferred intermediate of PGT124, and 9H+3L as an inferred intermediate of PGT121–123. First, we observed loss of neutralization for 3H+3L upon removal of individual glycan sites at N301 and N332, as previously reported (Sok et al., 2013), implying use of both glycan sites early in this lineage (Table S4). Neutralization was reduced after N301 removal for 32H+3L and 9H+3L with complete loss after N332 removal, suggesting a somewhat reduced dependence on N301 during affinity maturation relative to N332. A similar pattern was observed for other isolates (Sok et al., 2013). Strikingly, N137 removal resulted in enhanced neutralization for both inferred intermediate antibodies and for the affinity-matured antibodies (Table S4), suggesting that the N137 glycan plays a largely obstructive role. However, in the absence of the N332 glycan, it appears that the N137 glycan can play a positive binding role. If N332 and N137 are both eliminated, antibodies from the PGT121 family fail to neutralize virus. The overall conclusion is that the N332 glycan is preferentially used by all antibodies of the PGT121 lineage but that the N137 glycan can be utilized by PGT121–123 if N332 is absent (Table S5). Moreover, this effect is also observed to a lesser degree for N301 and N156 glycans that do not generally contribute to binding in the presence of N332 but become important for PGT121–123 in the absence of N332 (Table S4). In contrast, for the PGT124 branch, the N332 glycan appears to be sufficient for neutralization and contact with N137 is avoided (Tables S4 and S5). Thus, markedly different epitope recognition is observed for antibodies derived from the same germline lineage. With regard to the N301 glycan, PGT124 CDR H2 is shifted away from its equivalent position in

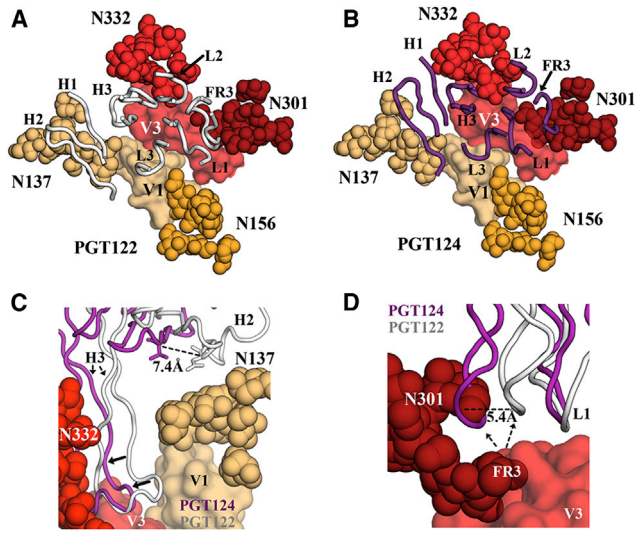

Figure 5. PGT122 Contacts Glycans at N137 and N301, but PGT124 Accommodates These Glycans without Forming Contacts

(A) The PGT122 epitope is composed of V1 and V3 regions from gp120, as well as four glycans at N137, N156, N301, and N332. The CDR loops and FR3 are shown in cartoon representation (in gray) (PDB ID: 4NCO).

(B) Superposition of PGT124 (in purple) on the PGT122 epitope.

(C) Although PGT124 seems capable of accommodating a glycan in the open face formed by H2 and H3, those loops appear to be shifted toward the center of the epitope when compared to the PGT122 paratope, thereby avoiding contacts with the N137 glycan.

(D) However, PGT124 is predicted to clash with the 301 glycan and presumably pushes this glycan away to access the protein surface below.

PGT122 (Figure 5C) and toward N301 glycan (Figure 5D). In fact, PGT124 would clash with N301 if it were to maintain the same orientation it adopts in the PGT122 complex. Thus, PGT124 appears to avoid this glycan consistent with apparent cleavage by EndoH in the presence of PGT124 and no visible electron density.

As previously observed, glycan arrays indicated that PGT121 binds biantennary complex glycans containing terminal sialic acid moieties with α-6 linkages (Julien et al., 2013c; Mouquet et al., 2012), but not high-mannose glycans (Figures 6A–6C). PGT128 and 2G12 only bind high-mannose glycans on glycan arrays (Calarese et al., 2003; Pejchal et al., 2011). In contrast, PGT124 does not bind any glycans on these arrays (Figures 6A–6C). The lack of complex glycan binding is consistent with the structural evidence that PGT124 does not interact with V1/V2 glycans, which are likely complex. Indeed, similar data were reported for 10-1074, a closely related somatic variant of PGT124 (Figure S1B) (Mouquet et al., 2012). However, lack of detectable high-mannose binding to PGT124 on the arrays is more puzzling but is consistent with weak interaction with the N332 glycan that requires cooperative interaction with the GDIR motif to attain high-affinity binding. For WEAU, one of the few HIV-1 strains in which N332A mutation does not abrogate PGT124 neutralization, virus produced in the presence of kifunensine, which results in only $Man_{8-9}GlcNAc_2$ glycoforms, is more sensitive to PGT124 neutralization than wild-type virus, suggesting that complex glycans are not required for PGT124 neutralization even in the absence of N332, in contrast to PGT121 (Figure S7).

PGT121–123 allosterically inhibit CD4 binding to gp120 by interacting with the V1/V2 loop (Julien et al., 2013c). To test whether this mechanism also applies to PGT124, we performed sequential ITC binding experiments in which CD4 was titrated into a solution containing full-length gp120 precomplexed with PGT124 or vice versa. We found no difference in PGT124 or CD4 binding whether or not the other was precomplexed with full-length gp120 (PGT124: Kd of 38 nM versus 34 nM precomplexed with CD4; CD4: Kd of 55 nM versus 50 nM precomplexed with PGT124). Thus, PGT124 does not inhibit gp120-CD4 binding, either allosterically or otherwise, which further highlights differences in epitope recognition compared to PGT121 (Figure S3E).

DISCUSSION

Following HIV-1 infection, a proportion of individuals develops potent broadly neutralizing antibody responses over time. Typically, sets of monoclonal antibodies can be isolated that consist of somatic variants arising from a single germline precursor, but individual variants can differ considerably in sequence, neutralization profiles, and breadth. Investigation of these somatic variants can aid in understanding what to expect from a vaccine-induced polyclonal antibody response to a given epitope and highlight features that might be gainfully incorporated into a vaccine immunogen and in vaccination strategies designed to elicit antibodies to that epitope.

To this end, we performed a structural study of members of the highly potent PGT124 family of bnAbs. PGT121, for example, protects against virus challenge at exceptionally low serum titers in macaque models (Moldt et al., 2012). Previous work also noted differences in glycan site recognition between somatic variants (Sok et al., 2014), and phylogenetic studies reported divergence in affinity maturation between PGT121–123 and 10-1074/PGT124 (Mouquet et al., 2012; Sok et al., 2013). We therefore investigated these phenotypic differences by comparing epitope recognition between somatic variants PGT122 and PGT124 in atomic detail.

The overall binding site architectures of the PGT124/10-1074, PGT121–123, and germline precursor antibodies are strikingly similar; all contain a closed face (Julien et al., 2013c; Mouquet et al., 2012) on one side of the paratope for binding the N332 glycan and similarly oriented long CDR loops that reach through to the protein surface below (Figure S1B). All antibodies also have an equivalent open face with a U-shaped depression; for PGT122, this face contacts surrounding glycans, whereas for PGT124, it enables avoidance of neighboring glycans. These observations suggest that, from the initial recombination event, the overall shape of the germline precursor is compatible with penetration of the glycan shield on the Env trimer in the region of N332 (Figure S1B). Indeed, the germline precursor already contains 8 of the 11 residues that are used by PGT124 to recognize the N332 glycan (5 residues) and the GDIR peptide sequence (6 residues) (Figure 4). A three amino acid insertion in FR L3, which occurred early in the maturation process, makes key contacts to the N332 glycan, highlighting its importance for the binding and neutralization by this antibody family (Sok et al., 2013).

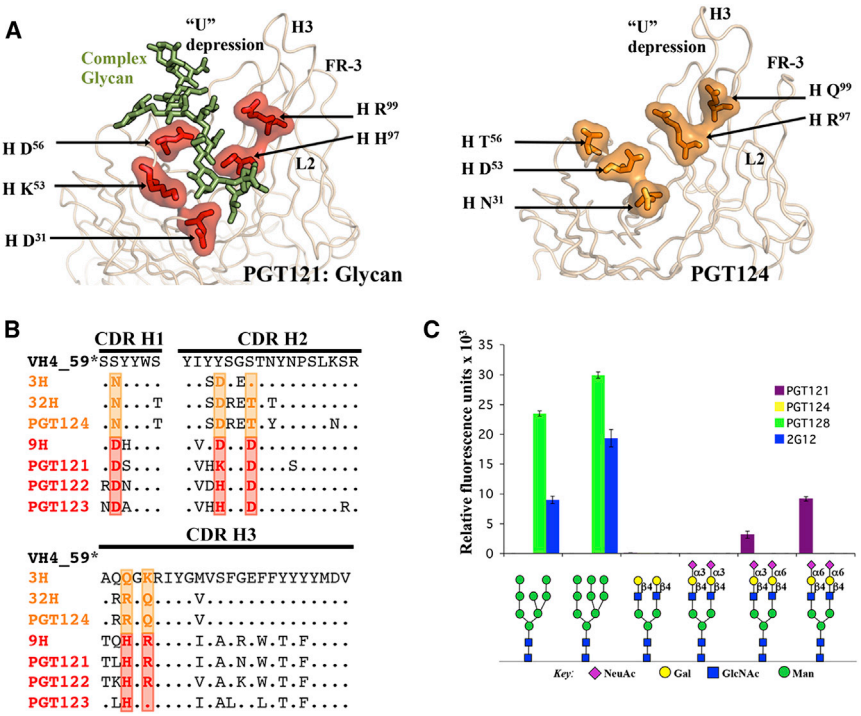

Figure 6. Evolution of Recognition of Complex Glycans by the PGT121 Family

(A) Key residues on PGT121 (Kabat numbering) that contact the complex glycan attached at N137 of gp120 V1 are represented in red as a stick and ball and are covered with its molecular surface on the ribbon representation of the antibody variable regions (left). Residues at equivalent positions on PGT124 are highlighted in orange (right).

(B) Sequence alignment for heavy-chain variable region for the germline precursor (GL) (asterisk indicates that the germline CDR H3 sequence is not used for the alignment because of ambiguity associated with D gene assignment), intermediate precursors (3H, 32H, and 9H), and mature antibodies of the PGT121 family (PGT121–124). Red boxes indicate residues involved in N137 glycan binding by PGT121, whereas orange boxes indicate the residues at equivalent positions on PGT124.

(C) Glycan arrays illustrate that PGT124, in contrast to PGT121, PGT128, or 2G12, does not bind either complex or high-mannose glycans with any demonstrable affinity (see also Figures S1, S3, and S7). Error bars, SD; n = 6; RFU, relative fluorescence units.

However, the structural analyses, as well as neutralization and binding assays, revealed a remarkable divergence in glycan epitope recognition by this antibody lineage that could have been driven by changes in the glycan sites over the course of chronic infection, although this hypothesis cannot be tested directly as longitudinal samples are not available. However, enhanced neutralization by all members of this lineage in the absence of the N137 glycan suggests that the initial encounter with this glycan was unfavorable, if it was present, but likely contributed to selecting the overall antibody shape required to bind the N332 glycan, penetrate through the glycan shield to access the V3 base, and avoid unfavorable contacts with other neighboring glycans. Following this initial event, antibody maturation appears to have proceeded along two different paths. Via the PGT124 route, affinity maturation appears to have focused on recognition on the V3 base and the N332 glycan. For PGT121–123, affinity maturation appears to have expanded the recognition to up to four glycans, including N137, depending upon isolate context, which likely could counter potential virus escape through deletion of the N332 glycan (Figure 7). Even though the PGT124 epitope is substantially smaller than PGT121–123, PGT124's potency and breadth match the other antibodies (Sok et al., 2014). One possible explanation is that interactions with the protein component substitute for binding to multiple glycans. Accordingly, the GDIR motif is just as important as the N332 glycan for binding and neutralization for most isolates (Figures 2D, 3E, S3B, and S3C). Thus, the single glycan at N332 is necessary but not sufficient because the GDIR motif is also required for PGT124 binding and neutralization.

Our observations also highlight the inherent flexibility in how glycans can serve as binding sites for antibodies as well as for other proteins. Furthermore, N137 glycan deletion in the presence of the N332 glycan enhances neutralization of BG505, indicating that this glycan can restrict antibody recognition. In contrast, deletion of both N137 and N332 totally abrogates PGT121–123 neutralization against the BG505 strain (Figure 7 and Table S4). Thus, the same glycan can participate in or shield a neutralizing epitope. For example, deletion of the N156 glycan has no effect on neutralization by any PGT121 lineage antibody except when N332 is absent, where some dependency is now observed (PGT122 and PGT123) (Table S4). In contrast, N332 makes productive contacts with all antibodies, confirming its role in the epitope core. The N301 glycan is important for neutralizing activities of the 3H precursor and, to a lesser extent, 9H and 32H precursors (Table S4). In contrast, in the absence of N332, PGT121 and particularly PGT122 show some dependency on N301, whereas deletion of both glycans completely abrogates binding of PGT123 (Table S4). In summary, several glycans may be involved in initiating an early PGT121 family response, but different maturation pathways result in divergent glycan recognition profiles. This complexity in glycan recognition may be generalized to other antibodies such as PG9 and PG16 (Pancera et al., 2013; Walker et al., 2009), which both recognize N156 and N160 in V1/V2, but PG9 has evolved a preference for N160, whereas PG16 favors N156 (McLellan et al., 2011; Pancera et al., 2013).

These results also have implications for protein-glycan recognition and vaccine design. Broader recognition of glycoproteins or glycopeptides can be achieved by focusing recognition on the conserved core of otherwise variable glycans. Second, because of such conserved features, neighboring glycans may be able to substitute for some variation in glycan location. Third, affinity can be enhanced by binding to multiple glycans even within a single binding site and also by latching on to the conserved regions of

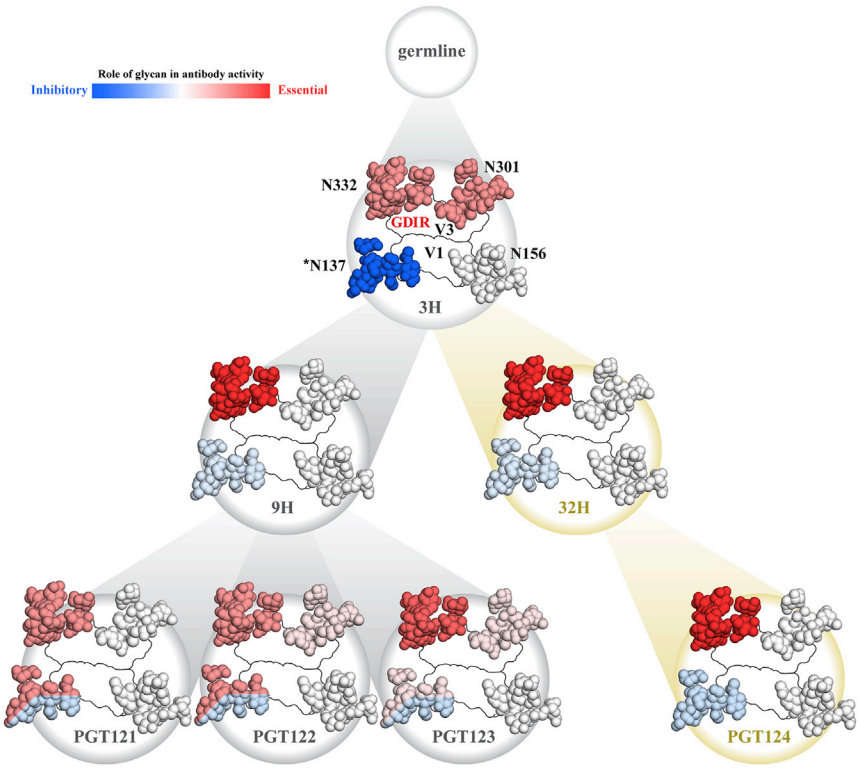

Figure 7. Summary of the Contributions of the N137, N156, N301, and N332 Glycans to Recognition of the BG505 Isolate by Antibodies of the PGT121 Lineage

Early precursors are highly dependent on the N301 and N332 glycans for neutralization and are negatively impacted by the presence of the N137 glycan (asterisk indicates that N137 glycan can play a double role in glycan recognition—first it can inhibit antibody binding by shielding the epitope, here represented in blue, and second, although it can still inhibit antibody binding to some extent, the N137 glycan can also be used by PGT121–123 to neutralize BG505 in the absence of N332, here represented in blue/red). Affinity maturation appears to create two distinct lineages that evolve separate dependencies on glycans that surround N332. N332 is the only critical glycan in the PGT124 epitope, whereas the N137 glycan contributes negatively to recognition by this antibody. Fold changes in neutralization IC_{50} for single and double glycan mutants (Table S4) were used to determine whether a glycan positively contributes to the epitope (decrease in neutralization IC_{50} upon removal) or contributes to shielding of the epitope (increase in neutralization IC_{50} upon removal). A relative scale for both positive and negative glycan contributions to the epitope was determined based on the extent of the change in neutralization IC_{50}. Interestingly, for PGT121–123, the N137 glycan contributes to shielding in the presence of N332 but is a critical part of the epitope in the absence of N332 (see also Table S4 and S5).

the protein, albeit even very short segments. For vaccine design, further considerations must be taken into account. For the PGT121 family, immunogens would first be designed to select for germline antibodies with relatively long CDR H3 lengths (24 amino acids) that could insert between the glycans and reach the underlying protein surface below. An appropriate antibody shape would be required for intimate binding of the N332 glycan (closed face in the PGT121 family), and another cavity (open face) to contact (PGT121–123) or avoid (PGT124) surrounding glycans. To facilitate initial engagement, an immunogen without the N137 glycan may enhance epitope recognition as illustrated for engagement of germline antibodies to the CD4 binding site by removal of a blocking glycan (Jardine et al., 2013). It is not yet clear whether removal of a blocking glycan would compromise selection of an appropriately shaped antibody. Following this initial selection event, modified immunogens would be used to drive clonal diversity of the selected antibody germline family that could include adding back or altering glycans to emulate events that likely occurs during virus evolution under immune pressure. To achieve a productive angle of approach of the antibody in the context of the Env trimer, the immunogen would likely require a native glycan shield or native-like Env structure to encourage accommodation of potentially obstructive neighboring glycans and drive somatic mutations to productively utilize neighboring glycans. Thus, these results provide insights into protein recognition of glycosylated proteins and demonstrate the remarkable ability of the human immune system to find and evolve multiple solutions for high-affinity antibody binding of complex epitopes so as to neutralize highly variable and highly glycosylated viruses, such as HIV.

EXPERIMENTAL PROCEDURES

Expression and Purification of Proteins

CD4 was expressed in *E. coli* BL-21 DE3* cells in LB media and purified by affinity chromatography followed by size exclusion chromatography (SEC). PGT124 Fab was produced in FreeStyle 293F cells (Invitrogen) and purified by affinity chromatography followed by cation exchange chromatography and SEC. JRCSF gp120 core was produced in FreeStyle 293S. Protein was purified using a GN Lectin column, followed by SEC. BG505 SOSIP.664 trimer was expressed in FreeStyle 293F or 293S cells and purified using a 2G12-coupled affinity matrix followed by SEC (Extended Experimental Procedures).

Formation of Protein Complexes, Crystallization, and Data Collection

Complexes were formed by combining gp120:ligands in a 1:1.2 molar ratio, followed by deglycosylation with Endoglycosidase H before being purified by SEC. Crystals of PGT124-gp120coremV3-CD4 ternary complex were obtained from 2.4 M $(NH_4)_2SO_4$, 0.1 M Tris (pH 8.0), and 13% glycerol that diffracted to 3.3Å resolution (Table S1). Unliganded PGT124 Fab crystals appeared from 20% (w/v) PEG 4000, 0.2 M $MgCl_2$, and 0.1 M Tris-HCl (pH 8.5) and diffracted to 2.5 Å (Extended Experimental Procedures and Table S1).

Structure Determination and Refinement

The unliganded PGT124 structure was solved by molecular replacement using Phaser with the PGT122 Fab structure (PDB 4JY5) as the initial model in which the CDR loops had been deleted. For the ternary complex, multiple components were used for phasing: CD4-gp120 (PDB ID:4JM2) and the high-resolution unliganded PGT124 Fab. Model building and refinement were carried out using Coot (Emsley and Cowtan, 2004) and Phenix (Adams et al., 2010),

respectively. Table S6 shows the components that were included in the final model. R_{cryst} and R_{free} for the unliganded structure are 23.5% and 26.7% and 21.0% and 26.3% for the complex (Table S1). Buried molecular surface areas were analyzed with the Molecular Surface Package (Connolly, 1993) using a 1.7 Å probe radius. The Fab residues were numbered according to Kabat (Martin, 1996), and gp120 is numbered following the Hxbc scheme (Ratner et al., 1987).

Isothermal Titration Calorimetry

ITC binding experiments were performed using a MicroCal Auto-iTC200 instrument (GE). All proteins were extensively dialyzed against a buffer containing 20 mM Tris and 150 mM NaCl (pH 7.4), and protein concentrations were adjusted and confirmed using calculated extinction coefficients and absorbance at 280 nm. In the syringe, ligand was either PGT124 Fab or sCD4 at concentrations ranging between 60 and 125 μM. The gp120 monomer was in the cell at concentrations ranging between 3.5 and10 μM. Two-protein binding experiments were performed as follows: cell at 25°C, 16 injections of 2.5 μl each, injection interval of 180 s, injection duration of 5 s, and reference power of 5 μcals. To perform sequential binding experiments, the mixed sample from the first titration was left in the cell, and the concentration of the HIV-1 component was recalculated based on the dilution from the first experiment (~88% of the initial concentration). Subsequently, either PGT124 Fab or sCD4 was added in a second titration. To calculate the affinity constants (K_D), the molar reaction enthalpy (ΔH) and the stoichiometry of binding (N), Origin 7.0 software was used by fitting the integrated titration peaks using a single-site binding model.

Antibody and Envelope Substitutions

Substitutions in the PGT124 paratope, the HIV-1 Env glycoprotein, and the JRCSFmV3 construct were introduced using QuikChange site-directed mutagenesis (Stratagene). Substitutions were verified by DNA sequencing (Retrogen).

Neutralization Assays

Neutralization activity of antibodies against pseudovirus in TZM-bl cells was determined as described previously (Li et al., 2005).

Electron Microscopy

PGT124 Fab in complex with BG505 SOSIP.664 gp140 produced in HEK293S cells were analyzed by negative stain EM. A 3 μl aliquot of 10 μg/ml of the complex was applied for 15 s onto a glow-discharged, carbon-coated 400 Cu mesh grid and stained with 2% uranyl formate for 20 s. Grids were imaged using a FEI Tecnai T12 electron microscope operating at 120 kV using 52,000× magnification and electron dose of 25 $e^{-}/Å^2$, resulting in a pixel size of 2.05 Å at the specimen plane. Images were acquired with a Tietz 4k × 4k CCD camera in 5° tilt increments from 0° to 55° at a defocus of 1,000 nm using LEGINON (Suloway et al., 2005).

Image Processing

Particles were picked automatically by using DoG Picker and put into a particle stack using the Appion software package (Lander et al., 2009; Voss et al., 2009). Initial reference-free 2D class averages were calculated using unbinned particles via the Xmipp Clustering 2D Alignment and sorted into 400 classes (Sorzano et al., 2010). Particles corresponding to the complexes were selected into a substack, and another round of reference-free alignment was carried out using Xmipp Clustering 2D alignment and IMAGIC software (van Heel et al., 1996). To generate an ab initio 3D starting model, a template stack of 120 images of 2D class averages was used with imposing C3 symmetry. This starting model was refined against 12,245 raw particles for 30 cycles using EMAN (Ludtke et al., 1999). The resolution of the final reconstruction was calculated to be 17.8 Å using an FSC cutoff of 0.5 (Figure S2).

Glycan Array Production

Glycan arrays were custom printed on a MicroGridII (Digilab) contact microarray robot equipped with StealthSMP4B microarray pins (Telechem) as previously described. Briefly, samples of each glycan were diluted to 100 μM in 150 NaPO4 buffer (pH 8.4). Aliquots of 10 μL were loaded in 384-well plates and imprinted onto NHS-activated glass slides (SlideH, Schott/Nexterion) with 7 arrays, each containing 6 replicates of each sample at both concentrations. Printed slides were humidified postprint for 1 hr and desiccated overnight. Remaining NHS-ester residues were quenched by immersing slides in 50 mM ethanolamine in 50 mM borate buffer (pH 9.2) for 1 hr. Blocked slides were washed with water, spun dry, and stored at room temperature until use.

Glycan Array Screening and Analyses

Antibodies were diluted to 30 μg/ml + 15 μg/ml anti-human-IgG-RPE (JacksonImmuno) in PBS + 0.05% Tween-20. The prepared mixture was incubated for 30 min on ice and incubated on the array surface in a humidified chamber for 1 hr. Slides were subsequently washed by successive rinses with PBS-T, PBS, and deionized H2O. Washed arrays were dried by centrifugation and immediately scanned for FITC and R-PE signal on a Perkin-Elmer ProScanArray Express confocal microarray scanner. Fluorescent signal intensity was measured using Imagene (Biodiscovery), and mean intensity minus mean background was calculated and graphed using MS Excel.

ACCESSION NUMBERS

Coordinates and structure factors for Fab PGT124 and its complex with gp120 and CD4 are deposited with the PDB under accession codes 4R26 and 4R2G, respectively. The Fab PGT124:SOSIP.664 trimer EM reconstruction is deposited in the EMDB under accession code EMD-2753. The nucleotide sequences for the antibodies 3L, 3H, 32H, 9H, PGT124HC, and PGT124LC are deposited with the GenBank under the accession numbers KM507475, KM507476, KM507477, KM507478, KM507479, and KM507480, respectively.

SUPPLEMENTAL INFORMATION

Supplemental Information includes Extended Experimental Procedures, seven figures, and six tables and can be found with this article online at http://dx.doi.org/10.1016/j.cell.2014.09.009.

AUTHOR CONTRIBUTIONS

Project design by F.G., D.S., A.B.W., D.R.B., and I.A.W.; X-ray work and analysis by F.G. and L.K.; EM work by H.J.K. and A.B.W.; glycan array work by R.M. and J.C.P.; mutational work by D.S. and K.F.S.-F.; manuscript written by F.G., D.S., L.K., A.B.W., D.R.B., and I.A.W. All authors were asked to comment on the manuscript. This is manuscript 26090 from The Scripps Research Institute.

ACKNOWLEDGMENTS

We are very grateful to N. Laursen and X. Dai for assistance with data processing; A. Irimia and A. Sarkar for assistance with glycan refinement; N. Laursen and R. Stanfield for helpful discussions; M. Elsliger for computer support; M. Deller and H. Tien for crystallization screening; C. Corbaci for help with preparing figures; and J.P. Verenini for manuscript formatting. X-ray data sets were collected at the Stanford Synchrotron Radiation Lightsource (SSRL), a Directorate of the SLAC National Accelerator Laboratory and an Office of Science User Facility operated for the U.S. Department of Energy (DOE) Office of Science by Stanford University. The SSRL Structural Molecular Biology Program is supported by the DOE Office of Biological and Environmental Research; NIH's National Center for Research Resources, Biomedical Technology Program (P41RR001209); and the National Institute of General Medical Sciences (NIGMS). Electron microscopy data were collected at the National Resource for Automated Molecular Microscopy (NRAMM) at the Scripps Research Institute, which is supported by US National Institutes of Health (NIH) through the National Center for Research Resources' P41 program (RR017573). This work was supported by the International AIDS Vaccine Initiative Neutralizing Antibody Center; by the Center for HIV/AIDS Vaccine Immunology and Immunogen Discovery (CHAVI-ID UM1 AI00663) (A.B.W., D.R.B., and I.A.W.), by the HIV Vaccine Research and Design (HIVRAD) program (P01 AI832362 and R37 AI36082) (J.P.M., A.B.W., and I.A.W.), by NIH R01 AI084817

(I.A.W.), by NIH R01 AI332932 (D.R.B.), and by the Joint Center of Structural Genomics (JCSG) funded by the NIH NIGMS Protein Structure Initiative (U54 GM094586) (I.A.W.).

Received: July 8, 2014
Revised: August 19, 2014
Accepted: September 4, 2014
Published: September 25, 2014

REFERENCES

Adams, P.D., Afonine, P.V., Bunkóczi, G., Chen, V.B., Davis, I.W., Echols, N., Headd, J.J., Hung, L.W., Kapral, G.J., Grosse-Kunstleve, R.W., et al. (2010). PHENIX: a comprehensive Python-based system for macromolecular structure solution. Acta Crystallogr. D Biol. Crystallogr. *66*, 213–221.

Barouch, D.H., Whitney, J.B., Moldt, B., Klein, F., Oliveira, T.Y., Liu, J., Stephenson, K.E., Chang, H.W., Shekhar, K., Gupta, S., et al. (2013). Therapeutic efficacy of potent neutralizing HIV-1-specific monoclonal antibodies in SHIV-infected rhesus monkeys. Nature *503*, 224–228.

Binley, J.M., Wyatt, R., Desjardins, E., Kwong, P.D., Hendrickson, W., Moore, J.P., and Sodroski, J. (1998). Analysis of the interaction of antibodies with a conserved enzymatically deglycosylated core of the HIV type 1 envelope glycoprotein 120. AIDS Res. Hum. Retroviruses *14*, 191–198.

Bonomelli, C., Doores, K.J., Dunlop, D.C., Thaney, V., Dwek, R.A., Burton, D.R., Crispin, M., and Scanlan, C.N. (2011). The glycan shield of HIV is predominantly oligomannose independently of production system or viral clade. PLoS ONE *6*, e23521.

Calarese, D.A., Scanlan, C.N., Zwick, M.B., Deechongkit, S., Mimura, Y., Kunert, R., Zhu, P., Wormald, M.R., Stanfield, R.L., Roux, K.H., et al. (2003). Antibody domain exchange is an immunological solution to carbohydrate cluster recognition. Science *300*, 2065–2071.

Chang, V.T., Crispin, M., Aricescu, A.R., Harvey, D.J., Nettleship, J.E., Fennelly, J.A., Yu, C., Boles, K.S., Evans, E.J., Stuart, D.I., et al. (2007). Glycoprotein structural genomics: solving the glycosylation problem. Structure *15*, 267–273.

Connolly, M.L. (1993). The molecular surface package. J. Mol. Graph. *11*, 139–141.

Dam, T.K., Roy, R., Das, S.K., Oscarson, S., and Brewer, C.F. (2000). Binding of multivalent carbohydrates to concanavalin A and Dioclea grandiflora lectin. Thermodynamic analysis of the ''multivalency effect''. J. Biol. Chem. *275*, 14223–14230.

Depetris, R.S., Julien, J.P., Khayat, R., Lee, J.H., Pejchal, R., Katpally, U., Cocco, N., Kachare, M., Massi, E., David, K.B., et al. (2012). Partial enzymatic deglycosylation preserves the structure of cleaved recombinant HIV-1 envelope glycoprotein trimers. J. Biol. Chem. *287*, 24239–24254.

Emsley, P., and Cowtan, K. (2004). Coot: model-building tools for molecular graphics. Acta Crystallogr. D Biol. Crystallogr. *60*, 2126–2132.

Jardine, J., Julien, J.P., Menis, S., Ota, T., Kalyuzhniy, O., McGuire, A., Sok, D., Huang, P.S., MacPherson, S., Jones, M., et al. (2013). Rational HIV immunogen design to target specific germline B cell receptors. Science *340*, 711–716.

Julien, J.P., Cupo, A., Sok, D., Stanfield, R.L., Lyumkis, D., Deller, M.C., Klasse, P.J., Burton, D.R., Sanders, R.W., Moore, J.P., et al. (2013a). Crystal structure of a soluble cleaved HIV-1 envelope trimer. Science *342*, 1477–1483.

Julien, J.P., Lee, J.H., Cupo, A., Murin, C.D., Derking, R., Hoffenberg, S., Caulfield, M.J., King, C.R., Marozsan, A.J., Klasse, P.J., et al. (2013b). Asymmetric recognition of the HIV-1 trimer by broadly neutralizing antibody PG9. Proc. Natl. Acad. Sci. USA *110*, 4351–4356.

Julien, J.P., Sok, D., Khayat, R., Lee, J.H., Doores, K.J., Walker, L.M., Ramos, A., Diwanji, D.C., Pejchal, R., Cupo, A., et al. (2013c). Broadly neutralizing antibody PGT121 allosterically modulates CD4 binding via recognition of the HIV-1 gp120 V3 base and multiple surrounding glycans. PLoS Pathog. *9*, e1003342.

Kabsch, W. (2010). XDS. Acta Crystallogr. Sect. D. Biol. Crystallogr. *66*, 125–132.

Koch, M., Pancera, M., Kwong, P.D., Kolchinsky, P., Grundner, C., Wang, L., Hendrickson, W.A., Sodroski, J., and Wyatt, R. (2003). Structure-based, targeted deglycosylation of HIV-1 gp120 and effects on neutralization sensitivity and antibody recognition. Virology *313*, 387–400.

Kong, L., Lee, J.H., Doores, K.J., Murin, C.D., Julien, J.P., McBride, R., Liu, Y., Marozsan, A., Cupo, A., Klasse, P.J., et al. (2013). Supersite of immune vulnerability on the glycosylated face of HIV-1 envelope glycoprotein gp120. Nat. Struct. Mol. Biol. *20*, 796–803.

Lander, G.C., Stagg, S.M., Voss, N.R., Cheng, A., Fellmann, D., Pulokas, J., Yoshioka, C., Irving, C., Mulder, A., Lau, P.W., et al. (2009). Appion: an integrated, database-driven pipeline to facilitate EM image processing. J. Struct. Biol. *166*, 95–102.

Li, M., Gao, F., Mascola, J.R., Stamatatos, L., Polonis, V.R., Koutsoukos, M., Voss, G., Goepfert, P., Gilbert, P., Greene, K.M., et al. (2005). Human immunodeficiency virus type 1 env clones from acute and early subtype B infections for standardized assessments of vaccine-elicited neutralizing antibodies. J. Virol. *79*, 10108–10125.

Ludtke, S.J., Baldwin, P.R., and Chiu, W. (1999). EMAN: semiautomated software for high-resolution single-particle reconstructions. J. Struct. Biol. *128*, 82–97.

Ma, B.J., Alam, S.M., Go, E.P., Lu, X., Desaire, H., Tomaras, G.D., Bowman, C., Sutherland, L.L., Scearce, R.M., Santra, S., et al. (2011). Envelope deglycosylation enhances antigenicity of HIV-1 gp41 epitopes for both broad neutralizing antibodies and their unmutated ancestor antibodies. PLoS Pathog. *7*, e1002200.

Martin, A.C. (1996). Accessing the Kabat antibody sequence database by computer. Proteins *25*, 130–133.

McLellan, J.S., Pancera, M., Carrico, C., Gorman, J., Julien, J.P., Khayat, R., Louder, R., Pejchal, R., Sastry, M., Dai, K., et al. (2011). Structure of HIV-1 gp120 V1/V2 domain with broadly neutralizing antibody PG9. Nature *480*, 336–343.

Moldt, B., Rakasz, E.G., Schultz, N., Chan-Hui, P.Y., Swiderek, K., Weisgrau, K.L., Piaskowski, S.M., Bergman, Z., Watkins, D.I., Poignard, P., and Burton, D.R. (2012). Highly potent HIV-specific antibody neutralization in vitro translates into effective protection against mucosal SHIV challenge in vivo. Proc. Natl. Acad. Sci. USA *109*, 18921–18925.

Mouquet, H., Scharf, L., Euler, Z., Liu, Y., Eden, C., Scheid, J.F., Halper-Stromberg, A., Gnanapragasam, P.N., Spencer, D.I., Seaman, M.S., et al. (2012). Complex-type N-glycan recognition by potent broadly neutralizing HIV antibodies. Proc. Natl. Acad. Sci. USA *109*, E3268–E3277.

Otwinowski, Z., and Minor, W. (1997). Processing of X-ray diffraction data collected in oscillation mode. Methods Enzymol. *276*, 307–326.

Pancera, M., Shahzad-Ul-Hussan, S., Doria-Rose, N.A., McLellan, J.S., Bailer, R.T., Dai, K., Loesgen, S., Louder, M.K., Staupe, R.P., Yang, Y., et al. (2013). Structural basis for diverse N-glycan recognition by HIV-1-neutralizing V1-V2-directed antibody PG16. Nat. Struct. Mol. Biol. *20*, 804–813.

Pejchal, R., Doores, K.J., Walker, L.M., Khayat, R., Huang, P.S., Wang, S.K., Stanfield, R.L., Julien, J.P., Ramos, A., Crispin, M., et al. (2011). A potent and broad neutralizing antibody recognizes and penetrates the HIV glycan shield. Science *334*, 1097–1103.

Ratner, L., Fisher, A., Jagodzinski, L.L., Mitsuya, H., Liou, R.S., Gallo, R.C., and Wong-Staal, F. (1987). Complete nucleotide sequences of functional clones of the AIDS virus. AIDS Res. Hum. Retroviruses *3*, 57–69.

Reeves, P.J., Callewaert, N., Contreras, R., and Khorana, H.G. (2002). Structure and function in rhodopsin: high-level expression of rhodopsin with restricted and homogeneous N-glycosylation by a tetracycline-inducible N-acetylglucosaminyltransferase I-negative HEK293S stable mammalian cell line. Proc. Natl. Acad. Sci. USA *99*, 13419–13424.

Sanders, R.W., Vesanen, M., Schuelke, N., Master, A., Schiffner, L., Kalyanaraman, R., Paluch, M., Berkhout, B., Maddon, P.J., Olson, W.C., et al. (2002). Stabilization of the soluble, cleaved, trimeric form of the envelope glycoprotein complex of human immunodeficiency virus type 1. J. Virol. *76*, 8875–8889.

Sok, D., Laserson, U., Laserson, J., Liu, Y., Vigneault, F., Julien, J.P., Briney, B., Ramos, A., Saye, K.F., Le, K., et al. (2013). The effects of somatic hypermutation on neutralization and binding in the PGT121 family of broadly neutralizing HIV antibodies. PLoS Pathog. *9*, e1003754.

Sok, D., Doores, K.J., Briney, B., Le, K.M., Saye-Francisco, K.L., Ramos, A., Kulp, D.W., Julien, J.P., Menis, S., Wickramasinghe, L., et al. (2014). Promiscuous glycan site recognition by antibodies to the high-mannose patch of gp120 broadens neutralization of HIV. Sci. Transl. Med. *6*, 236ra263.

Sorzano, C.O., Bilbao-Castro, J.R., Shkolnisky, Y., Alcorlo, M., Melero, R., Caffarena-Fernández, G., Li, M., Xu, G., Marabini, R., and Carazo, J.M. (2010). A clustering approach to multireference alignment of single-particle projections in electron microscopy. J. Struct. Biol. *171*, 197–206.

Suloway, C., Pulokas, J., Fellmann, D., Cheng, A., Guerra, F., Quispe, J., Stagg, S., Potter, C.S., and Carragher, B. (2005). Automated molecular microscopy: the new Leginon system. J. Struct. Biol. *151*, 41–60.

van Heel, M., Harauz, G., Orlova, E.V., Schmidt, R., and Schatz, M. (1996). A new generation of the IMAGIC image processing system. J. Struct. Biol. *116*, 17–24.

Voss, N.R., Yoshioka, C.K., Radermacher, M., Potter, C.S., and Carragher, B. (2009). DoG Picker and TiltPicker: software tools to facilitate particle selection in single particle electron microscopy. J. Struct. Biol. *166*, 205–213.

Walker, L.M., Phogat, S.K., Chan-Hui, P.Y., Wagner, D., Phung, P., Goss, J.L., Wrin, T., Simek, M.D., Fling, S., Mitcham, J.L., et al.; Protocol G Principal Investigators (2009). Broad and potent neutralizing antibodies from an African donor reveal a new HIV-1 vaccine target. Science *326*, 285–289.

Walker, L.M., Huber, M., Doores, K.J., Falkowska, E., Pejchal, R., Julien, J.P., Wang, S.K., Ramos, A., Chan-Hui, P.Y., Moyle, M., et al.; Protocol G Principal Investigators (2011). Broad neutralization coverage of HIV by multiple highly potent antibodies. Nature *477*, 466–470.